

Foundation for unbiased cross-validation of spatio-temporal models for species distribution modeling

Diana Koldasbayeva^{1,*} and Alexey Zaytsev¹

*diana.koldasbayeva@skoltech.ru

¹Skolkovo Institute of Science and Technology, Bolshoy Boulevard 30, bld. 1, 121205 Moscow, Russia

ABSTRACT

Species Distribution Models (SDMs) often suffer from spatial autocorrelation (SAC), leading to biased performance estimates. We tested cross-validation (CV) strategies - random splits, spatial blocking with varied distances, environmental (ENV) clustering, and a novel spatio-temporal method - under two proposed training schemes: LAST FOLD, widely used in spatial CV at the cost of data loss, and RETRAIN, which maximizes data usage but risks reintroducing SAC. LAST FOLD consistently yielded lower errors and stronger correlations.

Spatial blocking at an optimal distance (SP 422) and ENV performed best, achieving Spearman and Pearson correlations of 0.485 and 0.548, respectively, although ENV may be unsuitable for long-term forecasts involving major environmental shifts. A spatio-temporal approach yielded modest benefits in our moderately variable dataset, but may excel with stronger temporal changes. These findings highlight the need to align CV approaches with the spatial and temporal structure of SDM data, ensuring rigorous validation and reliable predictive outcomes.

1 Introduction

Species Distribution Modeling (SDM) is widely employed in ecology to understand biodiversity patterns and predict shifts in species ranges under changing environmental conditions. However, the validity of SDM predictions is based on careful handling of spatial autocorrelation (SAC), the phenomenon by which observations located closer together in space tend to exhibit greater similarity than those farther apart¹⁻⁴. SAC violates the assumption of independent observations in statistical analyses, potentially introducing biased parameter estimates, overoptimistic model performance, and misleading ecological inferences^{5,6}. As such, mitigating SAC in SDM has received growing attention, given its critical implications for conservation planning, species management, and climate change studies.

Cross-validation (CV) is widely recognized as a pivotal tool for evaluating predictive models, including those used in SDM^{7,8}. Traditional K -fold CV partitions data into K subsets (folds) randomly, iteratively using one subset for model testing while training on the remaining folds. Despite its popularity, this approach often overlooks SAC by randomly splitting data, thus allowing spatially correlated points to appear in both the training and test sets. Such overlap leads to inflated estimates of model accuracy as it fails to measure a model's ability to extrapolate to new, spatially distinct regions⁹⁻¹¹.

To address these limitations, spatial CV strategies explicitly partition data into spatially independent folds¹⁰⁻¹³. For instance, geographical blocking creates folds separated by a minimum distance that ideally matches or exceeds the autocorrelation range¹⁰. Environmental blocking clusters locations based on feature similarity rather than pure geographic distance, ensuring that training and test sets encompass distinct ranges of predictor variables^{10,11}. These methods yield more conservative, but arguably more realistic, estimates of predictive performance in spatially structured data. Nonetheless, optimal blocking distances or buffer sizes can be difficult to determine, and environmental blocking may overlook key geographic constraints, limiting its applicability in long-term forecasts under changing climate conditions¹⁴.

While spatial CV techniques represent a significant step forward, several gaps persist. First, SAC is rarely considered alongside temporal dependencies. Given the growing usage of SDMs to predict range shifts under climate change, it is critical to evaluate how well these models generalize across both space and time^{15,16}. Incorporating temporal dimensions into blocking strategies can help avoid overly optimistic performance estimates when projecting into future scenarios or unmeasured time periods. Second, many spatial CV studies rely on default model settings, such as employing Random Forest with a fixed number of trees^{10,13,17}, overlooking the importance of hyperparameter tuning for predictive performance^{18,19}. Failure to systematically optimize hyperparameters not only undermines model accuracy but also obscures the true capabilities of spatial CV methods.

Another underexplored consideration is how best to use training data once the folds have been defined. In the ecological

literature, the LAST FOLD strategy, in which the final fold alone is used for training, has gained popularity to preserve spatial independence at the expense of sacrificing a substantial portion of the data set¹¹. Conversely, the RETRAIN strategy leverages all available data for final model building but risks reintroducing SAC and biasing predictive metrics. To date, no comprehensive comparisons have systematically evaluated the trade-offs between these two training strategies for SDM, particularly under diverse spatial and temporal contexts.

In this study, we address these gaps by proposing a unified framework that systematically combines spatial, environmental, and temporal blocking with rigorous hyperparameter tuning across multiple machine learning (ML) models. We introduce a novel spatio-temporal CV method that accounts for the spatial and temporal variation, thereby offering a robust test of model generalizability in dynamic environments. In addition, we compare two distinct training strategies—LAST FOLD and RETRAIN - to elucidate their respective strengths and limitations in balancing SAC mitigation versus comprehensive data usage. Our experimental setup explores Random Forest, Gradient Boosting, and its variations (XGBoost, LightGBM), illustrating how methodical hyperparameter optimization can substantially improve predictive and consequently future quality.

Overall, our contributions are threefold:

- We systematically compare LAST FOLD and RETRAIN training strategies to highlight the trade-offs between maintaining spatial independence and leveraging maximum data for model training.
- We propose and empirically evaluate a new spatio-temporal cross-validation method for SDM, addressing the joint effects of spatial and temporal dependencies.
- We emphasize the importance of hyperparameter tuning within spatial CV frameworks, showing how thoughtful optimization can enhance reliability and ecological interpretability of SDMs.

By tackling these challenges, our work provides a practical and flexible framework for ecologists and data scientists aiming to generate robust SDMs under diverse environmental scenarios. We believe that these insights will advance the field's ability to make reliable ecological inferences and, ultimately, to forecast how species can change their geographic ranges in an era of rapid global change.

2 Methods

2.1 Pipeline

To construct a robust predictive model, we followed a systematic pipeline that included data collection, preprocessing, model selection, spatial cross-validation, hyperparameter tuning, and performance evaluation (Figure 1B).

Initially, we performed general workflow from SDM (Figure 1A). We collected species and environmental data, including the maximum temperature, the minimum temperature, and precipitation, for the years 1994-2018 based on occurrence points. These raw variables transformed into bioclimatic variables. To ensure temporal independence, the dataset was split into two time periods: in-sample and out-of-sample. Details are provided in Section 2.2.

To forecast species distributions, we selected ensemble-based models, including Random Forest and Gradient Boosting, with advanced variations of the latter, like XGBoost and LightGBM, due to their strong performance in ecological modeling tasks²⁰. These models were trained and validated using a range of spatial cross-validation strategies, incorporating spatial, environmental, and a novel spatio-temporal blocking methods featuring varying distances. The full details of these methods are provided in Section 2.5.

We employed a systematic random search algorithm to identify optimal model configurations for each CV strategy. Details on the hyperparameter search and selected configurations are presented in Section 2.6.

To assess model performance, we used Receiver Operating Characteristic Area Under the Curve (ROC AUC) as the primary metric. ROC AUC was chosen for its robustness in evaluating classification performance under imbalanced datasets, a common scenario in ecological modeling²¹. Mean Absolute Error (MAE), Pearson correlation, and Spearman correlation were used to compare spatial blocking strategies, evaluating consistency between cross-validation and out-of-sample testing.

2.2 Species data

Given our use of spatio-temporal validation and cross-validation methods, it is imperative to have species data spanning different time intervals. Consequently, we identify species that provide sufficient data for both classes (occurrence and absence) and cover a significant period. Researchers typically utilize datasets from previous work that are readily available for testing various methods - while in our work we propose a new one that allows for future detailed evaluation of methods aimed at correct spatio-temporal validation.

We split the data according to years: for the out-of-time validation, we used data from 1994 to 2002, which includes the species and the same variables as in the current prediction, and data from 2003 to 2018 for the in-sample data. However, in ML

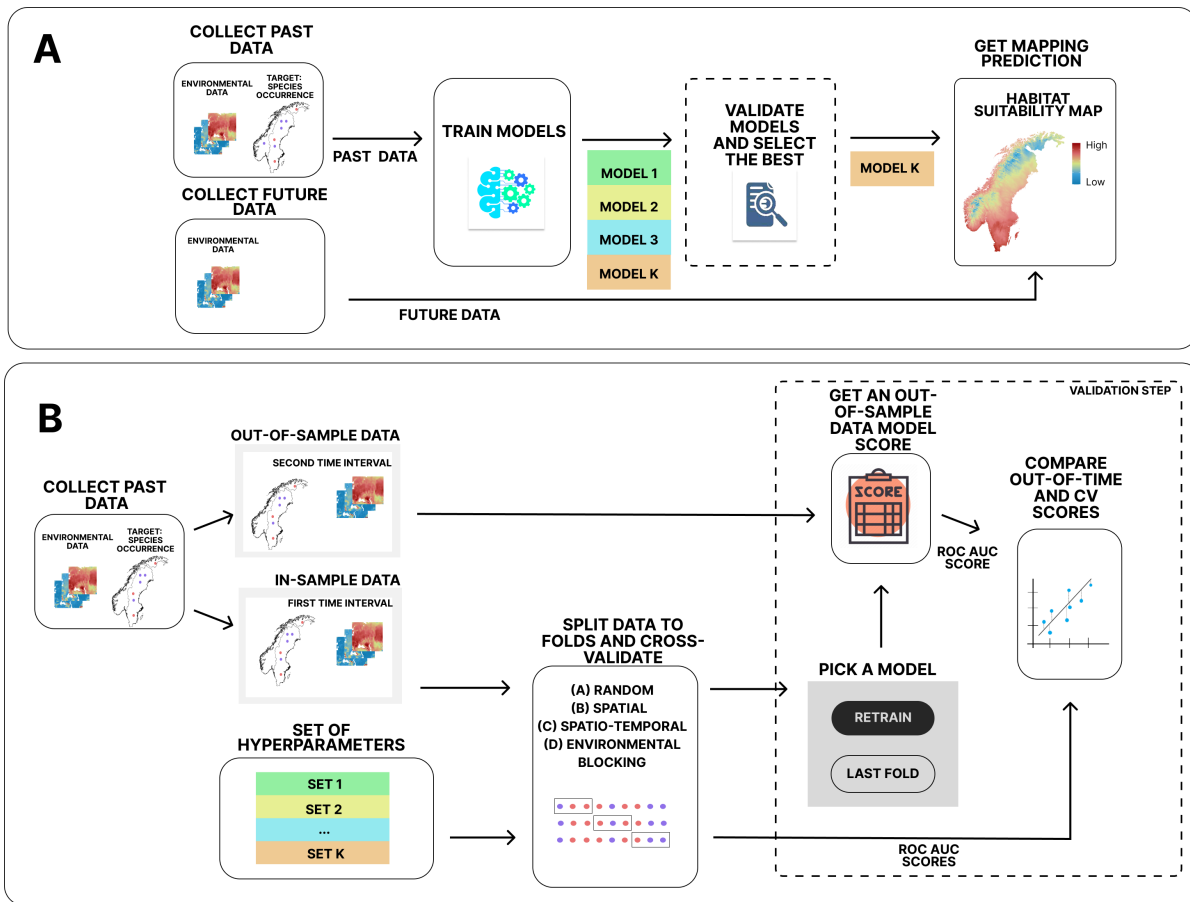


Figure 1. **A**) An SDM workflow example focusing on predicting species habitat suitability under future scenarios. **B**) Specific methodology of our study, including data collection across different time intervals, hyperparameter optimization, a comparison of two proposed training strategies and validation processes through both traditional and spatial cross-validation techniques.

generally test set includes later years to forecast future, our division strategically accounted for the prevalence of occurrence points in recent years, ensuring a meaningful split of past interval data as out-of-sample.

Study area The study area spans from 31°10' to 71°10' East longitude and from 3°55' to 55°20' North latitude, including regions within Norway and Sweden. It has 843215.4 km² area.

This region features a diverse climate, including temperate maritime conditions in the south and subarctic to Arctic climates in the north. Prominent geographic elements comprise extensive coastlines along the Baltic Sea and North Sea, as well as mountainous terrain in the western parts²².

Plant occurrence Due to a lack of temporal separation of similar research studies about species distribution, we collected data for species known as *Gentianella Campestris*. It is a small herbaceous biennial flowering plant in the *Gentianaceae* (gentian family) native to Europe. The coordinates of plant occurrence were collected from several publicly available sources related to citizen science projects from Global Biodiversity Information Facility database (GBIF)²³. The selection of species was performed according to the availability of absence data at available time intervals. The distribution of the appearance and absence points of this species is depicted in Figure 2.

Frequently, the absence of data is not allowed or limited in biodiversity databases. We used the data for 2003-2018 due to enough available data. For the current data, partial thinning was performed with 500 meters distance by *spThin* R Package²⁴, which means that we randomly deleted occurrence points that were located near 500 meters to avoid imbalanced and sampling bias problems.

2.3 Environmental predictors

We used 26 environmental predictors, such as bioclimatic variables, soil properties, and elevation. We did not perform feature selection due to our chosen models, which inherently possess the ability to deal with high-dimensional data and manage a mix

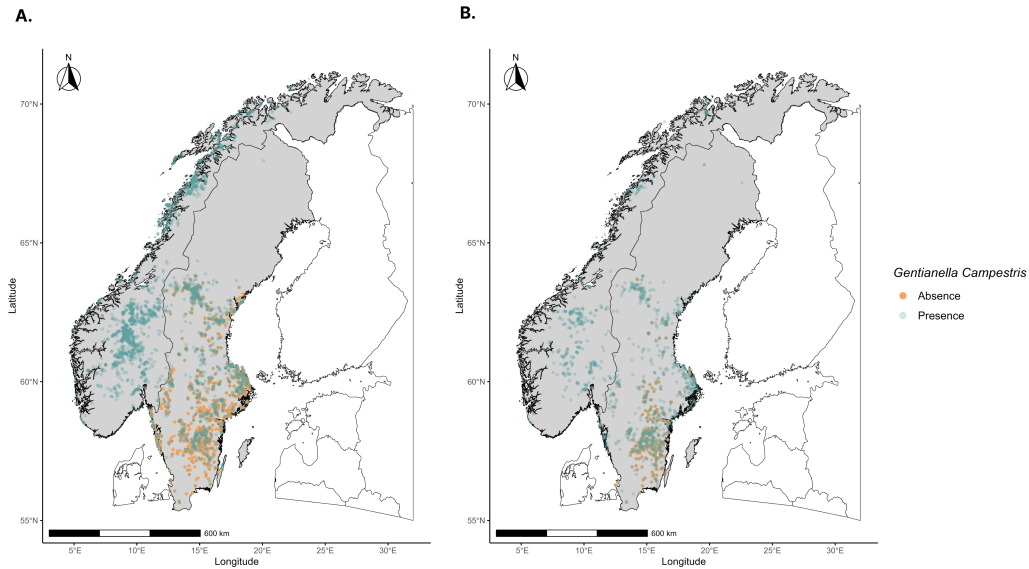


Figure 2. Spatial distribution of the target species: A) in-sample data for training the model; B) out-of-sample data for validation.

of informative and less relevant features.

We used `raster`²⁵, `rgdal`²⁶, `sf`²⁷, `terra`²⁸ R packages to prepare environmental data for modeling. The study region, defined using merged shapefiles, was used to mask and crop environmental rasters, including bioclimatic variables, soil properties, and elevation data. All layers were standardized to the WGS84 CRS and stacked into a single dataset. Table S1 (Supporting Information) lists the variables used in this study, and we refer the reader to the Worldclim²⁹ and SoilGrids³⁰ projects for detailed descriptions of variable derivation and calculation.

Climate data Environmental data are provided on the WorldClim database. The average minimum temperature (°C), average maximum temperature (°C), and total precipitation (mm) for the 1984-2018 time period were downloaded and converted in ASCII format using the R script. The resolution is 2.5 arc-minutes, according to the size of the studied area. We used `dismo`³¹ R package to convert all variables to bioclimatic variables, containing the average seasonal information relevant to the physiological characteristics of species.

We downloaded data by year and used two time intervals: 2003 - 2018 and 1984-2002. We averaged all bioclimatic parameters according to these periods. For spatio-temporal cross-validation, we averaged these bioclimatic variables for four periods: 2003-2006, 2007-2010, 2011-2014, and 2015-2018.

Soil data The soil data used in this study originates from the SoilGrids database. This global digital soil mapping system offers continuous data at various depths, providing spatial information about soil properties across the world at selected resolutions. It employs an ML approach to create continuous datasets based on 230000 soil profile observations from the WoSIS (World Soil Information Service) database with various environmental covariates.

From the extensive list of properties available through SoilGrids, we selected several key soil properties for our predictive modeling. These properties included the relative percentage of silt (Silt, %), sand (Sand, %), the volumetric fraction of coarse fragments (CF, %), bulk density of the fine earth fraction (bdod, cg/cm³), and soil organic carbon (SOC, g/kg) at a depth of 5–15 cm.

Elevation data was downloaded from the Worldclim database with the resolution of 2.5 arc-minutes.

2.4 Training strategies

Cross-validation for the identification of the best hyperparameters The RETRAIN strategy involves a two-step process aimed at optimizing the use of available data for model training. Initially, the training dataset $D = \{(\mathbf{x}_i, y_i)\}_{i=1}^N$ is partitioned into k -folds such that

$$D = \bigcup_{j=1}^k D_j, \quad D_j \cap D_{j'} = \emptyset \quad \text{for } j \neq j'.$$

For each fold j , a model M_θ with hyperparameters θ is trained on the training subset $D \setminus D_j$ and validated on the testing subset D_j . The optimal hyperparameters θ are determined by minimizing the average loss L across all folds:

$$\theta^* = \arg \min_{\theta} \frac{1}{k} \sum_{j=1}^k L(M_\theta, D_j),$$

the loss can be a mean squared error for a regression problem or one minus an ROC AUC score for a classification problem.

RETRAIN Once the best hyperparameters θ^* are identified, the model is retrained on the entire dataset D using these parameters to produce the final RETRAIN model:

$$M_{\text{final}} = M_{\theta^*}(D).$$

We note that θ^* can be different from the hyperparameters that provide the best error for a hold-out test sample, but we hope that they will be as close as possible.

This approach ensures that all available data contribute to the final model, potentially enhancing its robustness and predictive accuracy.

However, a notable limitation of the RETRAIN strategy is its disregard for spatial or temporal autocorrelation. By combining training and testing subsets during the retraining process, this method may lead to optimistic bias, particularly in datasets with strong SAC, where dependencies between data points inflate performance metrics. Nevertheless, RETRAIN remains a practical choice for scenarios where maximizing data utilization is prioritized over strict adherence to spatial or temporal independence.

LASTFOLD Instead of retraining the model on the entire dataset, as in the RETRAIN strategy, the LAST FOLD method trains the final model M_{final} using only the training subset of the last fold D_k and the optimized hyperparameters:

$$M_{\text{final}} = M_{\theta^*}(D_k).$$

This approach ensures that the final model reflects the spatial and temporal structure of the data, preserving dependencies within the last fold. Consequently, LAST FOLD is particularly suitable for scenarios where spatial and temporal autocorrelation plays a critical role, reducing the risk of overfitting to training data that differ from real-world test conditions. However, the method sacrifices some training data, as only a portion of the dataset is used for constructing the final model. This trade-off must be carefully considered when choosing the LAST FOLD strategy.

2.5 Methods of cross-validation

Random cross-validation Random k-fold cross-validation involves uniformly random splitting of a dataset into k subsets (folds) and using $k - 1$ folds for training and the remaining one for testing in each iteration. We repeated this process multiple times, and the performance metrics were averaged to evaluate the model's generalization ability. Random cross-validation was performed using R package `caret`³². In this method, all data were uniformly randomly split into five folds.

Spatial blocking Spatial cross-validation (CV) is a technique designed to account for spatial dependencies in data by dividing the study area into geographically distinct blocks³³.

To implement spatial blocking, the study area is divided into non-overlapping spatial blocks, where the size of the blocks determines the degree of spatial independence between training and validation folds. An optimal block size ensures sufficient spatial separation between blocks while maintaining enough data points in each fold for robust model training and validation¹⁰.

The optimal block size for spatial cross-validation was determined using the `blockCV` R package¹¹, specifically its `cv_spatial_autocor` function. This function automatically fits variograms to each continuous raster variable in the dataset to estimate the effective range of SAC. The SAC range represents the distance at which observations become spatially independent, based on the variogram analysis.

In our study, the SAC range was calculated as approximately 422 km. This distance was used as the optimal block size for spatial cross-validation, ensuring minimal SAC between training and validation blocks. To explore the effect of varying block sizes on model performance, we also tested smaller (200 km) and larger (600 km) block sizes. These blocks are referred to as **SP 200**, **SP 422**, and **SP 600**, respectively. Table 1 listed all types CV which were used in experiments.

Environmental blocking The objective of this method is to create clusters of data points that are homogeneous in terms of their environmental conditions while ensuring that each cluster contains a balanced representation of classes in the target variable. Environmental blocking is based on the K-mean clustering method. All features, including climate, soil, and elevation properties, were split into clusters. We chose the number of clusters by the elbow method³⁴. The proposed algorithm considered that each cluster must include both classes. We named this method **ENV**.

Table 1. CV types and their descriptions

Name	Description	Key details
Random	Random splitting	Cross-validation with random partitions, ignoring spatial structure.
SP 200	Spatial blocking (200 km)	Spatial blocks with a distance threshold of 200 km to separate folds.
SP 422	Spatial blocking (422 km)	Spatial blocks with a distance threshold of 422 km, aligned with SAC range.
SP 600	Spatial blocking (600 km)	Spatial blocks with a distance threshold of 600 km to separate folds.
ENV	Environmental blocking	Clustering data based on environmental similarity using K-means.
SPT 200	Spatio-temporal blocking (200 km)	Spatial blocks (200 km) combined with temporal folds (3 years).
SPT 422	Spatio-temporal blocking (422 km)	Spatial blocks (422 km) combined with temporal folds (3 years).
SPT 600	Spatio-temporal blocking (600 km)	Spatial blocks (600 km) combined with temporal folds (3 years).

Spatio-temporal blocking In adopting a temporal cross-validation strategy, our primary focus was on the temporal dynamics inherent in the data. Originally, we planned to assign a year’s worth of data to constitute a fold in the cross-validation process. However, due to the limitations of insufficient data for robust model training on an annual basis, we adjusted our approach. The data was partitioned into four distinct periods: 2003–2006, 2007–2010, 2011–2014, and 2015–2018. A more detailed partition (annual) would be less effective because climate predictors do not change significantly over short periods.

Similar to our spatial cross-validation methodology, within each of these time intervals, we further subdivided the data into five temporal folds, effectively implementing a temporal blocking scheme. This temporal blocking allowed us to create subsets of data that captured the evolving patterns and temporal dependencies within each designated period. Each of these temporal folds was then used iteratively as either the training or validation set in the cross-validation process. This process was repeated throughout 20 iterations, corresponding to the 5 spatial folds combined with the 4 distinct time intervals. By systematically cycling through the various temporal and spatial folds, we obtained a set of performance scores from each iteration, providing a comprehensive assessment of model performance across different temporal and spatial contexts. This method of cross-validation not only accounts for spatial variations but also ensures robust model validation across multiple spatial configurations and timeframes.

In this research, we refer to this methodology as **SPT 200**, **SPT 422**, and **SPT 600**, corresponding to 200 km, 422 km, and 600 km temporal block sizes, respectively.

2.6 Models

Classical ML algorithms tend to be used for tasks such as SDM with subsequent applications for identifying conservable or restorable areas³⁵. Random Forest and Boosting Decision Tree are some of the most popular tools in these research studies²⁰. Using the R packages `gbm`³⁶, `randomForest`³⁷, `xgboost`³⁸ and `lightgbm`³⁹, we adopted these models to predict the distribution of *Gentianella Campestris*.

We utilized a random search for hyperparameter tuning, selecting 120 hyperparameter sets at random from predefined ranges for each model. Table 2 lists the hyperparameters for each model.

Random Forest Random Forest is an ensemble learning method that constructs multiple decision trees during training and combines their predictions to produce a more robust and accurate model⁴⁰. It introduces randomness in the tree-building process by selecting random subsets of features and data points, reducing overfitting and improving generalization.

Gradient Boosting Gradient Boosting is a powerful ensemble learning method that builds a predictive model by combining the predictions of multiple weak learners, typically decision trees⁴¹. This method minimizes the loss function iteratively by adding new decision trees that focus on the mistakes made by the previous ensemble of trees. It sequentially fits new trees to the residuals of the previous predictions, gradually reducing prediction errors.

XGBoost One of the variations of Gradient Boosting models is XGBoost, which is widely used in various ML competitions and applications. Like other Gradient Boosting methods, XGBoost employs decision trees as weak learners and focuses on minimizing the loss function iteratively⁴². However, XGBoost stands out due to its unique features, such as a regularized objective function for improved model generalization, which helps prevent overfitting. Additionally, XGBoost includes enhancements like efficient handling of missing values, parallel processing for faster training, and advanced regularization techniques. The final prediction combines the individual forecastings from all the sequentially added decision trees.

LightGBM LightGBM is another variation of Gradient Boosting models that creates a predictive model through a collection of weak learners, often decision trees. Like other Gradient Boosting methods, LightGBM iteratively adds decision trees that focus on correcting the errors of previous trees, improving prediction accuracy as the boosting process continues⁴³. However,

Table 2. Hyperparameter ranges and types for each model.

Algorithm (package)	Hyperparameter	Values
Gradient Boosting (gbm)	n.tree	{50, 100, 250, 500, 750, 1000}
	shrinkage	{0.005, 0.01}
	interaction.depth	{3, 4, 5, 6}
	n.minobsinnode	{5, 10, 15, 20}
Random Forest (randomForest)	n.tree	{50, 100, 250, 500, 750, 1000}
	max depth	{3, 4, 5, 6, 7}
	min samples split	{5, 10, 15, 20}
XGBoost (xgboost)	n.rounds	{50, 100, 500, 1000}
	max.depth	{3, 5}
	eta	{0.01, 0.05, 0.1}
	subsample	{0.6, 0.7, 0.8}
	min.child.weight	{1, 5, 10}
	gamma	{0, 0.1, 1}
	colsample.bylevel	{0.6, 0.7, 0.8}
LightGBM (lightgbm)	num.iterations	{50, 100, 500, 1000}
	num.leaves	{10, 20, 30, 40}
	learning.rate	{0.01, 0.05, 0.1}
	subsample	{0.6, 0.7, 0.8}
	colsample.bytree	{0.6, 0.7, 0.8}

LightGBM stands out due to its unique approach to building trees, using a histogram-based learning algorithm for efficient training on large datasets and faster execution. By splitting the data into histograms, LightGBM significantly accelerates the algorithm, making it especially effective for large datasets.

2.7 Evaluation metrics

Having split our data into two temporal segments—namely, in-sample and out-of-sample data—we trained the models using the in-sample data. During training, cross-validation was applied to the in-sample data to tune hyperparameters and assess model performance. At this stage, we recorded the ROC AUC scores for each fold, as it is a widely used metric for evaluating binary classification performance.

After tuning the hyperparameters, we validated the models on the out-of-sample data and recorded the ROC AUC scores for this independent test set. The ROC AUC scores from the cross-validation phase and the out-of-sample validation were then compared to assess the consistency of the model’s performance across these phases.

To quantify the alignment between cross-validation and out-of-sample results, we computed the MAE, Pearson correlation, and Spearman correlation coefficients between the ROC AUC scores. The role of these metrics is detailed below:

2.7.1 Model evaluation

ROC AUC ROC AUC evaluates the model’s ability to distinguish between presence and absence during both cross-validation and out-of-sample testing. It measures the area under the ROC curve, which plots the true positive rate (sensitivity) against the false positive rate (1-specificity) at various threshold values. A higher ROC AUC score signifies better model discrimination, with a score of 1 indicating perfect discrimination and 0.5 representing random guessing^{44,45}.

2.7.2 Validation robustness

In this subsection, we introduce quality metrics suitable for evaluating the quality of scores obtained using a specific cross-validation strategy. We take into account that we are interested not only in a specific predicted quality value (we’ll have a biased value anyway) but as well in ranking models according to obtained scores. So, we assume that we have model scores $\hat{s} = \{\hat{s}_i\}_{i=1}^m$ obtained from a validation method and true scores obtained using a large separate test sample $s = \{s_i\}_{i=1}^m$. From these scores, we compute the vector of ranks $R(s)$, where instead of specific values, we have their corresponding ranks at a specific place of a vector.

MAE MAE measures the absolute difference between the ROC AUC scores from cross-validation and out-of-sample testing. This metric quantifies the average absolute difference between predicted and actual values⁴⁶. A lower MAE indicates that the

model’s predictions are closer to the true values, while a higher MAE signifies greater prediction errors:

$$\text{MAE}(\hat{\mathbf{s}}, \mathbf{s}) = \frac{1}{m} \sum_{i=1}^m |s_i - \hat{s}_i|.$$

Pearson Correlation Pearson correlation evaluates the linear relationship between the ROC AUC scores from the two phases. It calculates the strength and direction of the linear association between the scores. A Pearson correlation coefficient close to 1 indicates a strong positive linear relationship, close to -1 suggests a strong negative linear relationship and near 0 implies a weak or no linear relationship. It has the following form:

$$\rho_{\text{Pearson}}(\hat{\mathbf{s}}, \mathbf{s}) = \frac{\sum_{i=1}^m (\hat{s}_i - \bar{\hat{s}})(s_i - \bar{s})}{\sqrt{\sum_{i=1}^m (\hat{s}_i - \bar{\hat{s}})^2 \sum_{i=1}^m (s_i - \bar{s})^2}},$$

where $\bar{s} = \frac{1}{m} \sum_{i=1}^m s_i$ is a mean value of the vector \mathbf{s} , and $\bar{\hat{s}} = \frac{1}{m} \sum_{i=1}^m \hat{s}_i$.

Spearman Correlation Spearman Correlation, also known as Spearman’s rank correlation coefficient, measures the monotonic relationship between the quality scores from cross-validation and out-of-sample testing. Unlike Pearson Correlation, Spearman does not assume a linear relationship and can capture nonlinear monotonic associations. It has the following form where there are no ties:

$$\rho_{\text{Spearman}}(\hat{\mathbf{s}}, \mathbf{s}) = \rho_{\text{Pearson}}(R(\hat{\mathbf{s}}), R(\mathbf{s})) = 1 - \frac{6 \sum_{i=1}^m d_i^2}{m(m^2 - 1)},$$

where $d_i = R(\hat{\mathbf{s}})_i - R(\mathbf{s})_i$ is the difference between the two ranks of each observation.

This ρ_{Spearman} is particularly useful for evaluating consistency in rank-order performance, even in the presence of nonlinearity in the data.

3 Results

In this work, we conducted a comprehensive evaluation of eight distinct CV strategies — including seven spatial approaches designed to mitigate the impact of SAC — across four model types: Gradient Boosting, Random Forest, XGBoost, and LightGBM. For each model, we considered a grid of 120 hyperparameter configurations.

The primary challenge in validating models for spatial data lies in avoiding overoptimistic bias. In traditional ML workflows, significantly higher training or validation scores may indicate overfitting. However, in spatial contexts, such high scores can be misleading if training and validation folds share spatially correlated data. To address this, we assessed model performance using an independent test set drawn from a different time interval, thereby reducing the residual influence of SAC.

CV is commonly used for hyperparameter optimization and model validation. In the context of SDMs, spatial CV techniques are applied specifically to the training set to account for SAC. However, by default some workflows preserve only the final model from the last fold, effectively discarding potential insights from earlier folds. To address this limitation, we introduced two training strategies:

- **RETRAIN:** After identifying the best hyperparameters via CV, the model is retrained on the *entire* dataset (all folds combined).
- **LAST FOLD:** The model from the final fold of CV is used as the final model, prioritizing spatial independence but at the cost of discarding earlier-fold training data.

While the RETRAIN strategy leverages all available data to potentially improve model robustness, it does not strictly account for SAC in the retrained model. By contrast, the LAST FOLD strategy preserves spatial independence in the validation folds but sacrifices the additional training data from earlier folds.

To assess each approach’s ability to generalize, we tested all final models on an independent time-specific test set. We report the MAE as well as Spearman and Pearson correlation coefficients between ROC AUC scores. Two possible workflows are presented in Section 2.4, highlighting the trade-offs between RETRAIN and LAST FOLD.

3.1 Model evaluation

We evaluated the performance of ML models under different CV strategies, comparing the LAST FOLD and RETRAIN validation approaches. We examine both the average ROC AUC (Tables 3 and 4) and the maximum ROC AUC scores across all CV types (Tables 5 and 6).

Table 3. Comparison of ROC AUC under the LAST FOLD strategy. Each cell reports the average ROC AUC scores (\uparrow) across 120 hyperparameter configurations for each of the four models (Gradient Boosting, Random Forest, XGBoost, LightGBM).

CV	Gradient Boosting	Random Forest	XGBoost	LightGBM	Average
Random	0.725	0.723	0.736	0.744	0.732
SP 200	0.733	0.721	0.740	0.756	0.738
SP 422	0.751	0.752	0.759	0.756	0.755
SP 600	0.773	0.755	0.780	0.756	0.766
envBlock	0.716	0.731	0.726	0.745	0.730
SPT 200	0.705	0.688	0.693	0.689	0.694
SPT 422	0.706	0.678	0.696	0.689	0.692
SPT 600	0.722	0.698	0.707	0.702	0.707
Average	0.729	0.718	0.742	0.742	-

Table 4. Comparison of ROC AUC under the RETRAIN strategy. Each cell reports the average ROC AUC scores (\uparrow) across 120 hyperparameter configurations for each of the four models (Gradient Boosting, Random Forest, XGBoost, LightGBM).

CV	Gradient Boosting	Random Forest	XGBoost	LightGBM	Average
Random	0.733	0.727	0.745	0.756	0.740
SP 200	0.732	0.727	0.745	0.756	0.740
SP 422	0.733	0.725	0.743	0.756	0.739
SP 600	0.733	0.726	0.745	0.756	0.740
envBlock	0.733	0.727	0.744	0.756	0.740
SPT 200	0.732	0.726	0.744	0.756	0.740
SPT 422	0.733	0.726	0.744	0.756	0.740
SPT 600	0.732	0.726	0.744	0.756	0.740
Average	0.733	0.726	0.744	0.756	-

3.1.1 Average performance across CV types

Tables 3 and 4 show the average ROC AUC scores in all hyperparameter configurations for each model.

LAST FOLD Spatial blocking with optimal distance (SP 422) and SP 600 emerged as the top CV types, achieving the highest average ROC AUC values of 0.755 and 0.766, respectively. Random CV consistently underperformed, with an average ROC AUC of 0.732. Gradient Boosting and LightGBM demonstrated similar performance trends, while Random Forest and XGBoost were more sensitive to the CV strategy used.

RETRAIN Average ROC AUC values were generally higher under RETRAIN, particularly for SP 422, SP 600, and ENV. The CV types with the highest performance achieved values of between 0.739 and 0.740 across most models. The RETRAIN strategy showed more consistent performance across all CV types, likely due to the full data retraining step, which maximizes the available data for model training.

3.1.2 Best-Case performance

We also compare the obtained quality scores with the top one for each model by presenting the best scores for a validation for each of the four considered models. These scores are provided in Tables 5 and 6. We can get further insights into the maximum potential performance for each model under different CV types.

In LAST FOLD scenario XGBoost achieved the highest oracle ROC AUC (0.799) using SP 600, highlighting its ability to excel with larger spatial blocks. Similarly, for RETRAIN strategy the highest oracle ROC AUC was achieved by XGBoost 0.790 using SP 422, demonstrating its robustness under this CV strategy. In both cases Random Forest has the lowest scores.

Table 5. Maximum ROC AUC under the LAST FOLD strategy. Each cell reports the maximum ROC AUC scores (\uparrow) across all cross-validation strategies for each of the four models (Gradient Boosting, Random Forest, XGBoost, LightGBM).

CV	Gradient Boosting	Random Forest	XGBoost	LightGBM
Random	0.758	0.741	0.769	0.773
SP 200	0.754	0.741	0.769	0.783
SP 422	<u>0.773</u>	0.772	<u>0.786</u>	0.783
SP 600	0.790	<u>0.770</u>	0.799	0.783
envBlock	0.755	0.746	0.762	0.769
SPT 200	0.717	0.710	0.706	0.705
SPT 422	0.726	0.704	0.711	0.708
SPT 600	0.735	0.714	0.725	0.721
Best score	0.790	0.772	0.799	0.783

Table 6. Maximum ROC AUC under the RETRAIN strategy. Each cell reports the maximum ROC AUC scores (\uparrow) across all cross-validation strategies for each of the four models (Gradient Boosting, Random Forest, XGBoost, LightGBM).

CV	Gradient Boosting	Random Forest	XGBoost	LightGBM
Random	0.761	0.744	0.776	0.783
SP 200	0.761	0.744	0.777	0.783
SP 422	0.764	0.741	0.790	0.783
SP 600	0.765	0.740	0.777	0.783
envBlock	0.762	0.742	0.777	0.783
SPT 200	0.760	0.733	0.775	0.783
SPT 422	0.761	0.733	0.772	0.783
SPT 600	0.759	0.735	0.771	0.783
Best score	0.765	0.744	0.790	0.783

3.2 Validation robustness

3.2.1 LAST FOLD

The LAST FOLD strategy uses only the training data from the final fold of cross-validation, allowing it to reflect the real-world prediction task more conservatively. This approach inherently sacrifices some training data to prioritize validation fidelity. The corresponding results are shown in Figure 3 and detailed in Table 7, which compares the MAE, Pearson, and Spearman correlation coefficients across different cross-validation schemes and models, including Gradient Boosting, Random Forest, XGBoost, and LightGBM.

Top-Performing methods ENV and SP 422 emerged as the top-performing CV methods under the LAST FOLD strategy. ENV achieved the highest Pearson correlation (0.548), highlighting its ability to generalize effectively when environmental features are the primary drivers of species distribution. SP 422, with the highest Spearman correlation (0.485), demonstrated its effectiveness in accounting for SAC by aligning closely with the spatial structure of the data. Both methods achieved low MAE scores, with averages of 0.014 and 0.029, respectively. Notably, Gradient Boosting combined with SPT 422 achieved the lowest MAE across all configurations (0.010), showcasing its robust performance when spatio-temporal dependencies are explicitly considered.

Underperforming methods Random and SP 600 methods of CV performed poorly under the LAST FOLD strategy. Random cross-validation exhibited the highest average MAE (0.112) and negative correlations for both Pearson (-0.026) and Spearman (-0.014), underscoring its inability to account for spatial dependencies. This misalignment between cross-validation and out-of-sample validation is further illustrated in Figure 3, where Random CV demonstrates significant discrepancies between test and validation results. Similarly, SP 600, which uses overly large spatial blocks, resulted in negative Pearson (-0.279) and Spearman (-0.333) correlations, indicating that excessive block sizes fail to preserve meaningful spatial dependencies during model validation.

Model comparisons Across all CV strategies, Gradient Boosting consistently outperformed other models, achieving the lowest MAE values and higher correlations across most configurations. This highlights its robustness in handling complex interactions and dependencies within the data. However, other ensemble models, such as LightGBM and XGBoost, also demonstrated strong performance under optimal cross-validation schemes, particularly ENV and SP 422.

3.2.2 RETRAIN

The RETRAIN strategy leverages the entire dataset for final model training after cross-validation, making it an effective approach to utilize all available data. To evaluate its performance, we compared the consistency of ROC AUC scores between CV and out-of-sample testing using metrics such as MAE, Pearson and Spearman correlation. Results are visualized in Figure S1 (Supporting Information). The metrics for the models retrained on the entire dataset after CV are presented in Table S2 (Supporting Information).

Top-Performing methods The ENV and SP 422 approaches showed the strongest consistency, with low MAE values of 0.015 and 0.017, respectively. These results indicate that these strategies effectively maintain alignment between CV and out-of-sample performance. Furthermore, both ENV and SP 422 achieved highest average Pearson correlations (0.450 and 0.483, respectively) and average Spearman correlations (0.377 and 0.474, respectively), reinforcing their robustness in preserving performance rankings.

Underperforming methods In contrast, Random CV showed the weakest performance, with the highest average MAE (0.104) and negative Pearson and Spearman correlations (-0.022 and -0.056, respectively). These results highlight its inability to account for spatial dependencies, leading to poor generalization. Similarly, SP 600 showed suboptimal results with a moderate MAE of 0.033 and negative correlations (-0.283 Pearson, -0.318 Spearman), suggesting that overly large spatial blocks do not capture sufficient variability within the block.

Spatio-temporal blocking strategies demonstrated intermediate performance, with MAE values ranging from 0.016 to 0.042. The moderate correlations (Pearson: -0.008-0.205, Spearman: -0.065-0.098).

Model comparison Gradient Boosting again takes the lead in most RETRAIN configurations, though LightGBM and XGBoost are competitive. Random Forest shows lower performance in highly spatial or environmental scenarios, consistent with LAST FOLD results.

4 Discussion

4.1 Comparing training strategies

CV is a standard tool in ML for hyperparameter optimization, after which a final model is typically retrained on the full dataset to maximize data usage. In ecological studies, however, addressing SAC often necessitates spatially structured CV.

Table 7. Comparison of performance metrics under the LAST FOLD strategy. Each cell reports the Mean Absolute Error (\downarrow)—which we seek to minimize—and Pearson/Spearman correlation coefficients (\uparrow)—which we seek to maximize. Scores are averaged over 120 hyperparameter configurations for each of the four models (Gradient Boosting, Random Forest, XGBoost, LightGBM).

CV	Metric	Gradient Boosting	Random Forest	XGBoost	LightGBM	Average
Random	MAE \downarrow	0.129	0.105	0.113	0.099	0.112
	Pearson \uparrow	0.856	-0.053	-0.405	-0.500	-0.026
	Spearman \uparrow	0.854	-0.020	-0.418	-0.472	-0.014
SP 200	MAE \downarrow	0.079	0.084	0.070	0.053	0.072
	Pearson \uparrow	0.792	0.148	-0.347	-0.437	0.039
	Spearman \uparrow	0.768	0.171	-0.319	-0.464	0.039
SP 422	MAE \downarrow	0.034	0.024	0.032	0.027	0.029
	Pearson \uparrow	0.747	0.053	0.601	0.527	0.482
	Spearman \uparrow	0.823	0.062	0.572	0.482	0.485
SP 600	MAE \downarrow	0.039	0.043	0.043	0.026	0.038
	Pearson \uparrow	0.106	-0.153	-0.366	-0.703	-0.279
	Spearman \uparrow	-0.037	-0.241	-0.394	-0.658	-0.333
ENV	MAE \downarrow	0.014	0.014	0.017	0.011	0.014
	Pearson \uparrow	0.696	0.170	0.632	0.696	0.548
	Spearman \uparrow	0.726	0.026	0.453	0.450	0.414
SPT 200	MAE \downarrow	0.040	0.050	0.049	0.050	0.047
	Pearson \uparrow	0.307	0.103	0.353	0.688	0.363
	Spearman \uparrow	0.136	0.041	0.290	0.612	0.270
SPT 422	MAE \downarrow	0.010	0.039	0.019	0.020	0.022
	Pearson \uparrow	0.585	0.214	0.261	0.019	0.270
	Spearman \uparrow	0.528	0.230	0.210	-0.017	0.238
SPT 600	MAE \downarrow	0.070	0.081	0.032	0.069	0.063
	Pearson \uparrow	0.387	0.318	0.562	0.247	0.379
	Spearman \uparrow	0.360	0.183	0.572	0.407	0.381

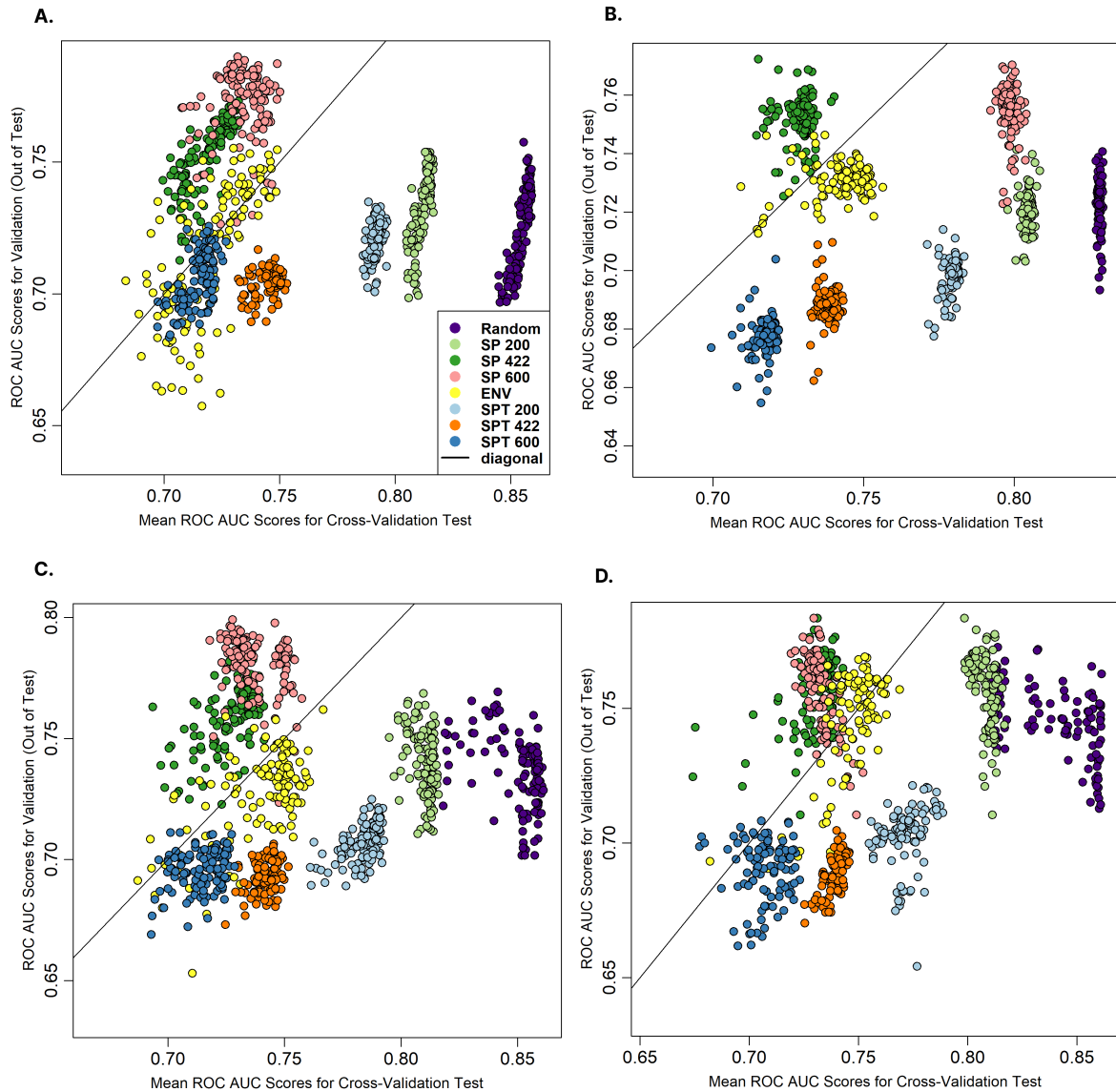


Figure 3. ROC AUC score comparison across models with LAST FOLD: This figure illustrates the performance of various models - A) Gradient Boosting, B) Random Forest, C) XGBoost, and D) LightGBM, each configured with distinct hyperparameters, through both cross-validation testing and out-of-sample validation.

Consequently, the LAST FOLD approach—training solely on the final fold—has been widely adopted to minimize leakage of SAC into the validation set^{10,13,33,47,48}.

Our results show that LAST FOLD generally outperformed RETRAIN across multiple CV methods. While RETRAIN theoretically leverages more training data, it does not fully eliminate the risk of spatial overlap between training and testing sets, leading to small correlations between training and test quality scores. By contrast, LAST FOLD yielded lower MAE and higher correlation coefficients in most configurations. For example, SP 422 obtained a Spearman correlation of 0.485 and a Pearson correlation of 0.482 under LAST FOLD, whereas ENV blocking achieved the highest Pearson correlation of 0.548. Such performance underscores the value of spatial independence in ecological modeling, where reliable extrapolation to new regions is more critical than slightly larger training datasets.

Random CV fared the worst in both strategies, displaying higher MAE (e.g., 0.112 under LAST FOLD) and negative correlations. This underlines the importance of incorporating spatial considerations in ecological contexts, where random splits do not adequately address SAC. Overall, our findings suggest that LAST FOLD is often the more dependable choice for real-world spatial predictions, despite its reduced training set size.

4.2 Evaluating spatial CV methods

Among the spatial CV methods examined, both SP 422 — a geographical blocking distance aligned with the SAC range—and ENV blocking outperformed other approaches. By aligning fold boundaries with key spatial scales, SP 422 effectively minimized autocorrelation between training and testing subsets, thereby improving generalization. ENV blocking, which groups data by environmental similarity, also performed well across most metrics, achieving a Pearson correlation of 0.548.

However, choosing an optimal distance threshold is paramount: blocking strategies set too small (e.g., SP 200) or too large (e.g., SP 600) failed to capture the spatial structure effectively, leading to inferior predictive performance (negative correlations for SP 600). These findings highlight the importance of conducting preliminary analyses such as variogram analysis to estimate SAC ranges accurately.

Despite its strengths, ENV blocking may face limitations in scenarios where environmental variables shift considerably over time or across regions—such as in climate change projections using CMIP6 data for future (e.g., 2040–2100) scenarios. In these cases, pure environmental clustering risks failing to account for geographic constraints¹¹. Consequently, for long-term predictions subject to large environmental changes, SP 422 (spatial blocking with optimal distance) may offer a more robust framework.

4.3 Suitability of spatio-temporal CV for SDM

Spatio-temporal blocking aims to address both spatial and temporal dependencies by combining spatial blocking with temporal segmentation. In our study, the spatio-temporal method with optimal distance (SPT 422) under the LAST FOLD strategy showed promising results for Gradient Boosting, achieving the lowest MAE (0.010) across all configurations. However, its correlation coefficients (Pearson: 0.270, Spearman: 0.238) were lower than those achieved by spatial blocking (SP 422) and ENV, suggesting that spatio-temporal CV may not always align as well with out-of-sample results.

One reason for this discrepancy may be the moderate temporal span in our data, which did not exhibit dramatic inter-annual climate variability. Consequently, spatio-temporal folds may have been too similar in climate attributes to reveal the full benefits of temporal blocking. In ecological or conservation modeling endeavors that encompass longer time frames (e.g., multi-decade intervals) or regions with highly variable climatic conditions, spatio-temporal CV may become more powerful. For instance, abrupt climate-driven shifts and species expansions or contractions could be better captured through extended temporal segmentation.

4.4 Model selection and hyperparameter tuning

While Random Forest remains one of the most popular models in SDM research due to its simplicity^{10,13,20,49–51}, our results indicate that boosting algorithms, such as Gradient Boosting, XGBoost, and LightGBM, consistently outperform Random Forest across multiple CV strategies. For example, Gradient Boosting achieved the lowest MAE (0.010) under spatio-temporal blocking and demonstrated robust performance across ENV and SP 422 methods.

Choosing the best model for a given data requires careful evaluation. Our findings highlight that different data and CV strategies may favor different models. Therefore, we recommend testing multiple algorithms and selecting the one that demonstrates the best performance under the chosen validation strategy.

Hyperparameter tuning also plays a critical role in model performance, yet it remains underexplored in SDM research. Our study used a random search approach to explore 120 hyperparameter configurations for each model, allowing us to identify optimal settings for each CV strategy. As shown in Figure 3, significant variability in model performance depending on the hyperparameter configuration. This underscores the importance of systematic hyperparameter optimization, which can significantly enhance model accuracy and generalizability in SDM applications.

5 Conclusion

Our work underscores the importance of carefully balancing data usage and spatial independence when validating SDMs. LAST FOLD emerged as a particularly robust training strategy, consistently mitigating SAC and offering more reliable performance estimates than RETRAIN—though RETRAIN may still be preferable for extremely limited datasets. We further demonstrated that spatial blocking (especially at an optimal distance) and environmental clustering can substantially improve SDM reliability, provided these methods are selected and configured based on the underlying data structures. The introduction of a spatio-temporal CV approach offers additional gains when temporal variability is significant, a scenario of growing relevance in climate change studies.

Moreover, our systematic hyperparameter optimization across multiple ML algorithms revealed that tuning plays a pivotal role in boosting predictive accuracy and ecological interpretability. By integrating robust spatial/temporal partitioning with careful model selection and tuning, researchers can better capture the complexities of biodiversity patterns, ultimately contributing to more informed conservation planning and effective responses to climate-driven range shifts.

References

1. Tobler, W. R. A computer movie simulating urban growth in the detroit region. *Econ. geography* **46**, 234–240 (1970).
2. Lennon, J. J. Red-shifts and red herrings in geographical ecology. *Ecography* **23**, 101–113 (2000).
3. Dormann, C. F. Effects of incorporating spatial autocorrelation into the analysis of species distribution data. *Glob. ecology biogeography* **16**, 129–138 (2007).
4. Ord, J. K. & Getis, A. Local spatial autocorrelation statistics: distributional issues and an application. *Geogr. analysis* **27**, 286–306 (1995).
5. Getis, A. Spatial autocorrelation. In *Handbook of applied spatial analysis: Software tools, methods and applications*, 255–278 (Springer, 2009).
6. Negret, P. J. *et al.* Effects of spatial autocorrelation and sampling design on estimates of protected area effectiveness. *Conserv. Biol.* **34**, 1452–1462 (2020).
7. Stone, M. Cross-validators choice and assessment of statistical predictions. *J. Royal statistical society: Ser. B (Methodological)* **36**, 111–133 (1974).
8. Geisser, S. The predictive sample reuse method with applications. *J. Am. statistical Assoc.* **70**, 320–328 (1975).
9. Dale, M. R. & Fortin, M.-J. *Spatial analysis: a guide for ecologists* (Cambridge University Press, 2014).
10. Roberts, D. R. *et al.* Cross-validation strategies for data with temporal, spatial, hierarchical, or phylogenetic structure. *Ecography* **40**, 913–929 (2017).
11. Valavi, R., Elith, J., Lahoz-Monfort, J. J. & Guillera-Arroita, G. blockcv: An r package for generating spatially or environmentally separated folds for k-fold cross-validation of species distribution models. *Methods Ecol. Evol.* **10**, 225–232 (2018).
12. Brenning, A. Spatial prediction models for landslide hazards: review, comparison and evaluation. *Nat. Hazards Earth Syst. Sci.* **5**, 853–862 (2005).
13. Ploton, P. *et al.* Spatial validation reveals poor predictive performance of large-scale ecological mapping models. *Nat. communications* **11**, 4540 (2020).
14. Santini, L., Benítez-López, A., Maiorano, L., Čengić, M. & Huijbregts, M. A. Assessing the reliability of species distribution projections in climate change research. *Divers. Distributions* **27**, 1035–1050 (2021).
15. Svenning, J.-C., Fløjgaard, C., Marske, K. A., Nógues-Bravo, D. & Normand, S. Applications of species distribution modeling to paleobiology. *Quat. Sci. Rev.* **30**, 2930–2947 (2011).
16. Elith, J. & Leathwick, J. R. Species distribution models: ecological explanation and prediction across space and time. *Annu. Rev. Ecol. Evol. Syst.* **40**, 677–697 (2009).
17. Wadoux, A. M.-C., Heuvelink, G. B., De Bruin, S. & Brus, D. J. Spatial cross-validation is not the right way to evaluate map accuracy. *Ecol. Model.* **457**, 109692 (2021).
18. Probst, P., Boulesteix, A.-L. & Bischl, B. Tunability: Importance of hyperparameters of machine learning algorithms. *The J. Mach. Learn. Res.* **20**, 1934–1965 (2019).
19. Probst, P., Wright, M. N. & Boulesteix, A.-L. Hyperparameters and tuning strategies for random forest. *Wiley Interdiscip. Rev. data mining knowledge discovery* **9**, e1301 (2019).
20. Pichler, M. & Hartig, F. Machine learning and deep learning—a review for ecologists. *Methods Ecol. Evol.* **14**, 994–1016 (2023).
21. Pecchi, M. *et al.* Species distribution modelling to support forest management. a literature review. *Ecol. Model.* **411**, 108817 (2019).
22. Ketzler, G., Römer, W. & Beylich, A. A. The climate of norway. *Landscapes landforms Nor.* 7–29 (2021).
23. GBIF.org. Gbif occurrence download (2022). Accessed: 2022-11-22.
24. Aiello-Lammens, M. E., Boria, R. A., Radosavljevic, A., Vilela, B. & Anderson, R. P. sphin: an r package for spatial thinning of species occurrence records for use in ecological niche models. *Ecography* **38**, 541–545 (2015).
25. Hijmans, R. J. *et al.* Package ‘raster’. *R package* **734**, 473 (2015).
26. Bivand, R. *et al.* Package ‘rgdal’. *Bind. for Geospatial Data Abstr. Libr. Available online: <https://cran.r-project.org/web/packages/rgdal/index.html> (accessed on 15 Oct. 2017)* **172** (2015).

27. Pebesma, E. J. *et al.* Simple features for r: standardized support for spatial vector data. *R J.* **10**, 439 (2018).
28. Hijmans, R. J. *et al.* Package ‘terra’. *Maintainer: Vienna, Austria* (2022).
29. Fick, S. E. & Hijmans, R. J. Worldclim 2: new 1-km spatial resolution climate surfaces for global land areas. *Int. journal climatology* **37**, 4302–4315 (2017).
30. Hengl, T. *et al.* Soilgrids250m: Global gridded soil information based on machine learning. *PLoS one* **12**, e0169748 (2017).
31. Hijmans, R. J., Phillips, S., Leathwick, J., Elith, J. & Hijmans, M. R. J. Package ‘dismo’. *Circles* **9**, 1–68 (2017).
32. Kuhn, M. *et al.* Package ‘caret’. *The R J.* **223** (2020).
33. Pohjankukka, J., Pahikkala, T., Nevalainen, P. & Heikkonen, J. Estimating the prediction performance of spatial models via spatial k-fold cross validation. *Int. J. Geogr. Inf. Sci.* **31**, 2001–2019 (2017).
34. Kodinariya, T. M., Makwana, P. R. *et al.* Review on determining number of cluster in k-means clustering. *Int. J.* **1**, 90–95 (2013).
35. Beery, S., Cole, E., Parker, J., Perona, P. & Winner, K. Species distribution modeling for machine learning practitioners: A review. In *ACM SIGCAS conference on computing and sustainable societies*, 329–348 (2021).
36. Greenwell, B., Boehmke, B., Cunningham, J., Developers, G. & Greenwell, M. B. Package ‘gbm’. *R package version 2* (2019).
37. Liaw, A., Wiener, M. *et al.* Classification and regression by randomforest. *R news* **2**, 18–22 (2002).
38. Chen, T., He, T., Benesty, M. & Khotilovich, V. Package ‘xgboost’. *R version* **90**, 1–66 (2019).
39. Shi, Y. *et al.* *lightgbm: Light Gradient Boosting Machine* (2024). R package version 4.3.0.99.
40. Breiman, L. Random forests. *Mach. learning* **45**, 5–32 (2001).
41. Friedman, J. H. Greedy function approximation: a gradient boosting machine. *Annals statistics* 1189–1232 (2001).
42. Chen, T. & Guestrin, C. Xgboost: A scalable tree boosting system. In *Proceedings of the 22nd ACM SIGKDD international conference on knowledge discovery and data mining*, 785–794 (2016).
43. Ke, G. *et al.* Lightgbm: A highly efficient gradient boosting decision tree. *Adv. neural information processing systems* **30** (2017).
44. Bradley, A. P. The use of the area under the roc curve in the evaluation of machine learning algorithms. *Pattern recognition* **30**, 1145–1159 (1997).
45. Shabani, F., Kumar, L. & Ahmadi, M. Assessing accuracy methods of species distribution models: Auc, specificity, sensitivity and the true skill statistic. *Glob. J. Human-Social Sci. B Geogr. Geo-Sciences, Environ. Sci. & Disaster Manag.* **18** (2018).
46. Willmott, C. J. & Matsuura, K. Advantages of the mean absolute error (mae) over the root mean square error (rmse) in assessing average model performance. *Clim. research* **30**, 79–82 (2005).
47. Mila, C., Mateu, J., Pebesma, E. & Meyer, H. Nearest neighbour distance matching leave-one-out cross-validation for map validation. *Methods Ecol. Evol.* **13**, 1304–1316 (2022).
48. Koldasbayeva, D. *et al.* Challenges in data-driven geospatial modeling for environmental research and practice. *Nat. Commun.* **15**, 10700 (2024).
49. Schratz, P., Muenchow, J., Iturrutxa, E., Richter, J. & Brenning, A. Hyperparameter tuning and performance assessment of statistical and machine-learning algorithms using spatial data. *Ecol. Model.* **406**, 109–120 (2019).
50. Adhikari, P., Lee, Y. H., Poudel, A., Hong, S. H. & Park, Y.-S. Global spatial distribution of chromolaena odorata habitat under climate change: Random forest modeling of one of the 100 worst invasive alien species. *Sci. Reports* **13**, 9745 (2023).
51. Maglietta, R. *et al.* Environmental variables and machine learning models to predict cetacean abundance in the central-eastern mediterranean sea. *Sci. Reports* **13**, 2600 (2023).

6 Code availability

For the data, preprocessing and modelling details to reproduce the calculations, we refer the reader to the repository of the project https://github.com/Disha0903/spBlock_cv.

7 Author contributions statement

D.K. and A.Z. developed the experimental pipeline; D.K. collected the data, conducted the experiments, and drafted the manuscript; A.Z. provided supervision throughout the project; Both A.Z. and D.K. jointly analyzed the results and critically reviewed the manuscript.

8 Additional information

Competing interests

The authors declare no competing financial interests.

Supporting Information

Table S1. Description of used variables

Parameter	Full Name	Description	Source
BIO1	Annual Mean Temperature	Average of the maximum and minimum temperatures of a year	WorldClim
BIO2	Mean Diurnal Range	Mean of the difference of the monthly maximum and minimum temperature	WorldClim
BIO3	Isothermality	Magnitude of the the day-to-night temperatures oscillation relative to the summer-to-winter (annual) oscillations	WorldClim
BIO4	Temperature Seasonality	The amount of temperature variation over averaged years	WorldClim
BIO5	Max Temperature of Warmest Month	The maximum monthly temperature occurrence averaged over years	WorldClim
BIO6	Min Temperature of Coldest Month	The minimum monthly temperature occurrence averaged over years	WorldClim
BIO7	Temperature Annual Range	A measure of temperature variation over years range	WorldClim
BIO8	Mean Temperature of Wettest Quarter	Mean temperatures that prevail during the wettest season	WorldClim
BIO9	Mean Temperature of Driest Quarter	Mean temperatures that prevail during the driest season	WorldClim
BIO10	Mean Temperature of Warmest Quarter	Mean temperatures that prevail during the warmest quarter	WorldClim
BIO11	Mean Temperature of Coldest Quarter	Mean temperatures that prevail during the coldest quarter	WorldClim
BIO12	Annual Precipitation	Sum of all total monthly precipitation	WorldClim
BIO13	Precipitation of Wettest Month	Precipitation of Wettest Month	WorldClim
BIO14	Precipitation of Driest Month	The total precipitation that prevails during the driest month	WorldClim
BIO15	Precipitation Seasonality	The variation in monthly precipitation totals over the course of the years	WorldClim
BIO16	Precipitation of Wettest Quarter	Total precipitation that prevails during the wettest quarter	WorldClim
BIO17	Precipitation of Driest Quarter	Total precipitation that prevails during the driest quarter	WorldClim
BIO18	Precipitation of Warmest Quarter	Total precipitation that prevails during the warmest quarter	WorldClim
BIO19	Precipitation of Coldest Quarter	Total precipitation that prevails during the coldest quarter	WorldClim
Elevation	Elevation	SRTM elevation data	WorldClim
silt	Silt	Proportion of silt particles in the fine earth fraction	SoilGrids
sand	Sand	Proportion of sand particles in the fine earth fraction	SoilGrids
bdod	Bulk Density of Fine Earth	Bulk density of the fine earth fraction	SoilGrids
soc	Soil Organic Carbon	Soil organic carbon content in the fine earth fraction	SoilGrids

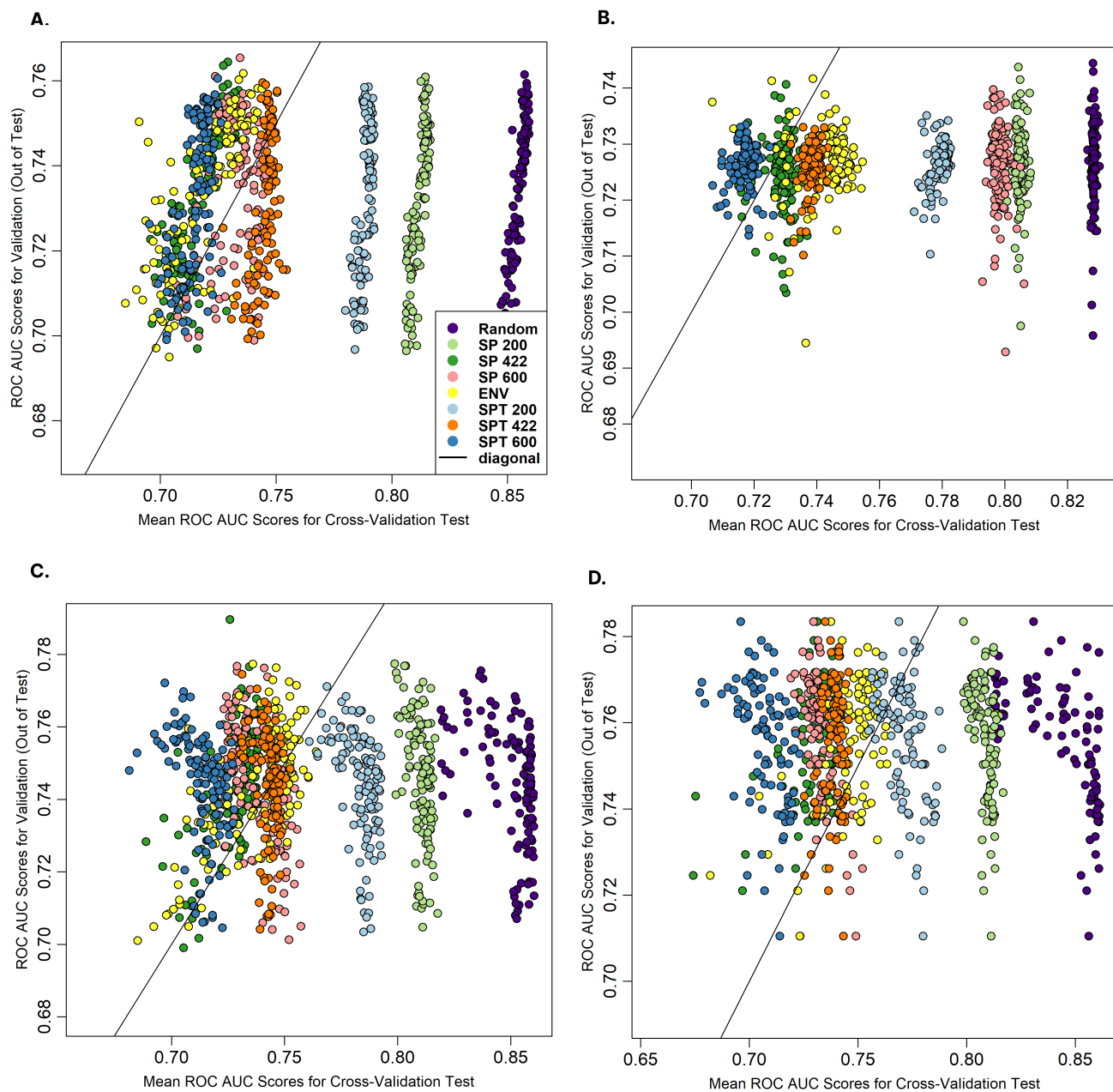


Figure S1. ROC AUC score comparison across models with RETRAIN: This figure illustrates the performance of various models - A) Gradient Boosting, B) Random Forest, C) XGBoost, and D) LightGBM, each configured with distinct hyperparameters, through both cross-validation testing and out-of-sample validation.

Table S2. Comparison of performance metrics under the RETRAIN strategy. Each cell reports the Mean Absolute Error (\downarrow)—which we seek to minimize—and Pearson/Spearman correlation coefficients (\uparrow)—which we seek to maximize. Scores are averaged over 120 hyperparameter configurations for each of the four models (Gradient Boosting, Random Forest, XGBoost, LightGBM).

CV	Metric	Gradient Boosting	Random Forest	XGBoost	LightGBM	Average
Random	MAE \downarrow	0.121	0.102	0.105	0.087	0.104
	Pearson \uparrow	0.907	0.049	-0.441	-0.604	-0.022
	Spearman \uparrow	0.884	0.051	-0.474	-0.686	-0.056
SP 200	MAE \downarrow	0.080	0.078	0.065	0.053	0.069
	Pearson \uparrow	0.849	0.053	-0.449	-0.437	0.004
	Spearman \uparrow	0.811	0.072	-0.423	-0.464	-0.001
SP 422	MAE \downarrow	0.017	0.007	0.017	0.027	0.017
	Pearson \uparrow	0.796	-0.024	0.634	0.527	0.483
	Spearman \uparrow	0.816	-0.035	0.632	0.482	0.474
SP 600	MAE \downarrow	0.015	0.072	0.020	0.026	0.033
	Pearson \uparrow	0.212	-0.150	-0.490	-0.703	-0.283
	Spearman \uparrow	0.025	-0.114	-0.527	-0.658	-0.318
ENV	MAE \downarrow	0.017	0.017	0.012	0.013	0.015
	Pearson \uparrow	0.741	-0.032	0.656	0.436	0.450
	Spearman \uparrow	0.761	-0.053	0.537	0.263	0.377
SPT 200	MAE \downarrow	0.016	0.013	0.014	0.019	0.016
	Pearson \uparrow	0.535	0.381	-0.266	0.168	0.205
	Spearman \uparrow	0.449	0.279	-0.322	-0.013	0.098
SPT 422	MAE \downarrow	0.019	0.010	0.032	0.048	0.027
	Pearson \uparrow	0.619	0.136	-0.400	-0.388	-0.008
	Spearman \uparrow	0.576	0.130	-0.513	-0.453	-0.065
SPT 600	MAE \downarrow	0.056	0.053	0.039	0.018	0.042
	Pearson \uparrow	0.637	0.392	-0.432	-0.444	0.038
	Spearman \uparrow	0.571	0.356	-0.493	-0.434	0.000